

A98-25060**AIAA-98-1768****THE RESPONSE OF COMPOSITE CYLINDRICAL SHELLS WITH CUTOUTS AND
SUBJECTED TO INTERNAL PRESSURE AND AXIAL COMPRESSION LOADS**

Mark W. Hilburger *
University of Michigan
Ann Arbor, MI 48109-2118

James H. Starnes Jr. †
NASA Langley Research Center
Hampton, VA 23681-0001

Anthony M. Waas ‡
University of Michigan
Ann Arbor, MI 48109-2118

Abstract

Results from an analytical study of the response of composite shells with cutouts and subjected to internal pressure and axial compression are presented. The analytical results are obtained using a geometrically nonlinear finite element code. Results for axial compression and combined internal pressure and axial compression are presented. The effects of varying internal pressure and cutout size on the prebuckling, buckling, and post-buckling responses of the shell are described. Results indicate that the nonlinear interaction between the in-plane load distribution and the out-of-plane displacements near the cutout can significantly influence the structural response of the shell. The results also indicate that these local load distributions and displacements can be affected by the size of the cutout and the internal pressure load.

Introduction

Many modern aerospace shell structures are designed to support combinations of internal pressure and mechanical loads during their service life. With the increasing need to produce lighter weight aerospace structures, the use of advanced composite materials has become more common in the design of these structures. During operation, flight loads and internal cabin pressure are present in all commercial transport aircraft. Some of these loads may be compressive loads and, thus, it is necessary to investigate the buckling characteristics of these structures. In addition, designers will

often need to incorporate cutouts or openings in the structure to serve as doors, windows, or access ports. It has been shown by a number of authors that a cutout in a shell structure subjected to axial compression can cause a significant reduction in the buckling load of the shell (e.g., Ref. 1-4). The local response near the cutout in a compression-loaded shell is strongly influenced by the local displacement gradients and the internal load distribution. These local displacements and internal load distribution can be affected by the size of the cutout. Recent studies of the response of cylindrical shells with longitudinal cracks and subjected to internal pressure and axial compression loads (e.g., Ref. 5) indicate that the interaction between the internal pressure load and the axial compression load can have a significant effect on the local response of the structure.

The results of an analytical study of the response of composite cylindrical shells with cutouts and subjected to internal pressure and axial compression are presented. First, the governing parameters for the buckling of cylindrical shells with a cutout will be defined. The governing parameters will be used to develop the results of a parametric study presented in the paper. These parameters will help provide insight into the effects of changing geometric and laminate parameters on the buckling response of shells. The parametric study will include three cutout sizes and five internal pressure levels to determine the effects of varying the cutout size and internal pressure loads on the compression response. The predicted results are characterized by load-shortening response curves and contour plots of shell displacements and stress resultants. Finally, design curves based on classical parameters for the buckling of shells with cutouts and subjected to internal pressure and axial compression are presented.

*Ph.D. Candidate, Composite Structures Laboratory, Department of Aerospace Engineering. Student Member, AIAA.

†Head, Structural Mechanics Branch. Fellow, AIAA.

‡Associate Professor, Composite Structures Laboratory, Dept. of Aerospace Engineering. Member AIAA. Copyright ©1998 by Mark W. Hilburger. Published by the American Institute of Aeronautics and Astronautics, Inc. with permission.

Classical Buckling Parameters

Nondimensional parameters governing the buckling of shells with cutouts were derived by Hilburger⁴ and are summarized herein. The governing equations for the buckling of anisotropic thin elastic shells were derived from the Donnell-Mustari-Vlasov nonlinear equations in terms of curvilinear coordinates using the method of adjacent equilibrium. A nondimensionalization procedure was applied to the governing equations producing a set of nondimensional parameters in terms of shell and cutout geometric parameters and laminate stiffnesses. The nondimensionalization procedure introduced the geometric parameters of the cutout into the equations with the following set of nondimensional coordinates,

$$X = \frac{x}{a} \text{ and } \Theta = \frac{\theta}{b}. \tag{1}$$

In the case of a circular cylindrical shell, x and θ represent the axial and circumferential coordinates, respectively, and a and b are the characteristic axial and circumferential dimensions of the cutout, respectively (see figure 1). After a significant amount of algebraic manipulation, the nondimensional transverse equilibrium equation and the compatibility equation take the following forms, respectively:

$$\begin{aligned} \alpha_b^2 \frac{\partial^4 w}{\partial X^4} + 4\alpha_b \gamma_b \frac{\partial^4 W}{\partial X^3 \partial \Theta} + 2\beta \frac{\partial^4 W}{\partial X^2 \partial \Theta^2} + 4 \frac{\delta_b}{\alpha_b} \frac{\partial^4 W}{\partial X \partial \Theta^3} \\ + \frac{1}{\alpha_b^2} \frac{\partial^4 W}{\partial \Theta^4} \sqrt{12} C \frac{\partial^2 \Phi}{\partial X^2} - K_x \pi^2 \frac{\partial^2 W}{\partial X^2} \\ - K_\theta \pi^2 \frac{\partial^2 W}{\partial \Theta^2} - 2 \frac{K_{x\theta} \pi^2}{\alpha_b^2} \frac{\partial^2 W}{\partial X \partial \Theta} = 0 \end{aligned} \tag{2}$$

and

$$\begin{aligned} \alpha_m^2 \frac{\partial^4 \Phi}{\partial X^4} + 2\alpha_m \gamma_m \frac{\partial^4 \Phi}{\partial X^3 \partial \Theta} + 2\mu \frac{\partial^4 \Phi}{\partial X^2 \partial \Theta^2} \\ + 2 \frac{\delta_m}{\alpha_m} \frac{\partial^4 \Phi}{\partial X \partial \Theta^3} + \frac{1}{\alpha_m^2} \frac{\partial^4 \Phi}{\partial \Theta^4} = \sqrt{12} C \frac{\partial^2 W}{\partial X^2} \end{aligned} \tag{3}$$

where Φ is a stress resultant function, and W is a nondimensional buckling displacement. The remaining parameters in Equation 2 are nondimensional bending parameters and buckling coefficients defined by

$$\alpha_b = \frac{b}{a} \left(\frac{D_{11}}{D_{22}} \right)^{1/4} \tag{4}$$

$$\beta = \frac{D_{12} + 2D_{66}}{\sqrt{D_{11} D_{22}}} \tag{5}$$

$$\gamma_b = \frac{D_{16}}{(D_{11}^3 D_{22})^{1/4}} \tag{6}$$

$$\delta_b = \frac{D_{26}}{(D_{11} D_{22}^3)^{1/4}} \tag{7}$$

$$K_x = \frac{N_x^0 b^2}{\pi^2 \sqrt{D_{11} D_{22}}} \tag{8}$$

$$K_\theta = \frac{N_\theta^0 a^2}{\pi^2 \sqrt{D_{11} D_{22}}} \tag{9}$$

$$K_{x\theta} = \frac{N_{x\theta}^0 b^2}{\pi^2 (D_{11} D_{22}^3)^{1/4}} \tag{10}$$

where D_{11} , D_{12} , D_{22} , D_{16} , D_{26} , and D_{66} are the shell bending stiffnesses found in classical laminated shell theory. N_x^0 , N_θ^0 , and $N_{x\theta}^0$ are the prebuckling in-plane stress resultants. The remaining parameters in Equation 3 are nondimensional membrane parameters and a cutout or curvature parameter, C , in terms of shell membrane stiffnesses A_{11} , A_{12} , A_{22} , A_{16} , A_{26} , and A_{66} . In the special case of balanced symmetric laminates with A_{16} and A_{26} equal to zero, these parameters are

$$\alpha_m = \frac{b}{a} \left(\frac{A_{11}}{A_{22}} \right)^{1/4} \tag{11}$$

$$\mu = \frac{A_{11} A_{22} - A_{12}^2 - 2A_{12} A_{66}}{2A_{66} \sqrt{A_{11} A_{22}}} \tag{12}$$

$$C = \frac{b^2}{R} \left[\frac{A_{11} A_{22} - A_{12}^2}{12 \sqrt{A_{11} A_{22} D_{11} D_{22}}} \right]^{1/2} \tag{13}$$

and $\gamma_m = 0$ and $\delta_m = 0$.

In the context of this paper, in which shells are subjected to internal pressure loading, P_{int} , it is useful to introduce the relation, $N_\theta^0 = P_{int} R$. This relation is derived from the membrane solution for a circular cylindrical shell subjected to internal pressure.

Cylinder Models and Analysis Methods

Cylinder Model

The STAGS (SStructural Analysis of General Shells) finite element analysis code⁶ was used to predict the response of the shells. A typical finite element model of the shells analyzed in this study is described in figure 1. The shell has a radius of 8.0 inches and is 16.0 inches long. The shells have an 8-ply [$\pm 45/0/90$]_s quasi-isotropic wall lamination. The ply thickness was assumed to be 0.005 inches resulting in a total laminate thickness of 0.04 inches. The lamina properties are summarized in Table 1. A square cutout is located at $\theta = 0^\circ$, at the shells mid-length. The cutouts considered in this study include 0.5-in by 0.5-in, 1.0-in by 1.0-in, and 1.5-in by 1.5-in square cutouts. The axial and circumferential dimensions of the cutout are denoted by a and b , respectively, as indicated in the figure. An idealized version of typical experimental boundary conditions were included in the model by constraining circumferential and radial degrees of freedom v and w , respectively, in regions of the cylinder $0.0\text{-in} \leq x \leq 1.0\text{-in}$ and $15.0\text{-in} \leq x \leq 16.0\text{-in}$ as illustrated in figure 1. The resulting has an unsupported length of 14.0 inches.

The loading conditions studied include axial compression and combined axial compression and internal pressure. For the axial compression cases, a compression load was applied to the shell by a uniform axial displacement. For the combined internal pressure and axial compression cases, the pressure load was applied to the shell first, and then an axial compression load was applied to the pressurized shell. Pressure levels equal to 5.0 psi, 10.0 psi, 20.0 psi, 30.0 psi, and 50.0 psi are applied to the shell for the combined load cases. The internal pressure was simulated by applying a uniform lateral pressure to the shell wall and an axial tension load to the end of the shell. Multi-point constraints were applied to the ends of the shell to enforce uniform displacement.

Nonlinear Analysis Methods

The quasi-static compression response of the shells was determined using a standard arc-length projection method⁷ in STAGS. The arc-length method is often sufficient for predicting results beyond instability points in the response. However, for cases where the standard arc-length method failed to converge to solutions beyond instability points, a nonlinear transient analysis method⁸ was employed. The transient analysis was initiated at an unstable equilibrium point just beyond the instability point by applying an increment in the end-shortening displacement. The transient analysis was continued until the kinetic energy in the system dissipated to a negligible level. A load relaxation procedure was applied to the system to establish a stable equilibrium state from which a quasi-static analysis could be resumed.

Results and Discussion

Results from a numerical study of the response of quasi-isotropic laminated shells with cutouts are presented. Two loading conditions were considered in this study and include axial compression only, and combination internal pressure and axial compression loads. Results have been generated for cutouts at the shell mid-length including 0.5-in by 0.5-in, 1.0-in by 1.0-in, and 1.5-in by 1.5-in square cutouts. Results have been generated for internal pressure loads of 5.0 psi, 10.0 psi, 20.0 psi, 30.0 psi, and 50.0 psi. First, results from a representative shell are presented to identify typical response characteristics of a shell with a cutout and subjected to axial compression. Results illustrating the effects of internal pressure on the compression response are presented. Finally, design curves are presented summarizing the effects of internal pressure on the initial buckling loads of shells with square cutouts.

Axial Compression Loads

Results from a quasi-isotropic $[\pm 45/0/90]_s$ shell with a 1.0-in by 1.0-in square cutout is presented to identify typical response characteristics of a compression-loaded shell with a cutout. The load-shortening response curve is given in figure 2a as an overall guide to the compression response. Extensive postbuckling response is indicated in the figure by a number of stable and unstable segments in the load-shortening results. The initial buckling point is labeled A and the additional extreme points are labeled B, C, D, etc. The post buckling response includes both stable segments (e.g., B-C, D-E) and unstable segments (e.g., A-B, C-D, E-F) as shown in the figure. Segments A-B and C-D are associated with unstable local buckling events that occur near the cutout. These buckling events result in large out-of-plane deformations and rapidly varying stress gradients near the cutout. Stable postbuckling segments B-C and D-E are accompanied by an increase in the magnitude of the local deformations in the shell near the cutout. Global collapse of the shell occurs at point E and the unstable collapse response is represented by segment E-F. The collapse response is characterized by a significant reduction in load and the development of the general instability mode in the shell. The load-time history of the collapse response is shown in figure 2b. The slope of each adjacent stable equilibrium segment of the response curve decreases as loading continues in the postbuckling range indicating a reduction in the effective axial compression stiffness of the shell. This decrease is due to the increasingly large deformations that develop in the shell throughout the compression response.

Deformation patterns corresponding to selected extreme points on the load-shortening response curve are shown in figure 3a-3f. Figure 3a shows the displacements associated with the initial buckling point A, consisting of an elliptical shaped inward buckle at the cutout with the semi-major axis aligned in a helical or skew direction. The postbuckling deformation pattern associated with point B consists of large elliptical shaped buckles on either side of the cutout. Deformation patterns in figures 3c, and 3d indicate that as the postbuckling response progresses, the elliptical buckles in the shell become increasingly well defined and the buckle pattern rotates counter-clock-wise around the cutout. Figure 3e shows an intermediate deformation pattern associated with point E* during the collapse response of the shell. The deformation pattern indicates that additional buckles propagate around the circumference of the shell during the response until the general instability collapse mode forms, shown in figure 3f.

Contour plots of axial and circumferential stress resultants corresponding to buckling point A in figure 2a

are shown in figure 4a and 4b, respectively. The results indicate that rapidly varying stress gradients form near the cutout and quickly decay to far-field values away from the cutout. In addition, the results indicate that regions of in-plane biaxial compression form near the cutout. These regions of destabilizing stresses couple with the out-of-plane deformations near the cutout causing the local buckling response. In-plane stress resultants associated with global collapse configuration are shown in figure 5a and 5b. The stress contours indicate that significant stress redistribution occurs as a result of the large out-of-plane deformations that develop.

Results indicate that variations in the size of the cutout can have a significant effect on the compression response of a shell with a cutout. Figure 6 shows the load-shortening relations for shells with 0.5-in by 0.5-in, 1.0-in by 1.0-in and 1.5-in by 1.5-in square cutouts. The results indicate that the magnitude of the initial buckling load decreases as the cutout size increases. The values of the normalized buckling loads are 0.83, 0.56 and 0.45 for the 0.5-in by 0.5-in, 1.0-in by 1.0-in and 1.5-in by 1.5-in square cutouts, respectively. An increase in the size of the cutout results in larger prebuckling displacements near the cutout. These larger displacements result in significant stress redistribution away from the cutout leading to an overall weakening of the shell at lower applied loads. For shells with 1.0-in by 1.0-in and 1.5-in by 1.5-in cutouts, the initial buckling response results in a stable local postbuckling state, and additional load can be applied to the shell before the overall collapse occurs. For the 0.5-in by 0.5-in square cutout, the initial local buckling response seemed to be enough of a disturbance to the shell to cause the general collapse of the shell.

Internal Pressure and Axial Compression Loads

The effects of internal pressure on the compression response of a shell with a 1.0-in by 1.0-in square cutout are summarized in figure 7a and 7b. The results indicate that the first local buckling loads increase with an increase in the internal pressure. The values of the normalized local buckling loads for the 1.0-in by 1.0-in cutout and internal pressure levels of 0.0 psi, 10.0 psi, 30.0 psi and 50.0 psi are 0.56, 0.64, 0.70 and 0.79, respectively. The internal pressure delays the formation of the regions of destabilizing biaxial compression near the cutout (as discussed in the axial compression only case) and, hence, delays the onset of the local buckling of the shell. Results indicate that an increase in the internal pressure results in a decrease in the magnitude of the postbuckling load reduction. This trend continues until a value of internal pressure is reached for which

the first local buckling response does not include an unstable local buckling response. For these results, shells with an internal pressure greater than or equal to 30 psi have a stable first local buckling response accompanied by a gradual development of large out-of-plane deformations and rapidly varying stress gradients near the cutout. The results indicate that the general instability load for the shells increases and the magnitude of the collapse load reduction decreases as the level of internal pressure increases.

A typical example of the initial postbuckling deformation pattern for a shell with a 1.0-in by 1.0-in cutout and subjected to 30 psi of internal pressure and axial compression is shown in figure 8a. The results indicate that the internal pressure significantly influences the shell deformations compared to the results for axial compression only. The displacements are characterized by large out-of-plane local bending of the axially aligned edges of the cutout. Figure 8b shows the general instability collapse mode for the same shell and indicates that an increase in the internal pressure results in an increase in the number of axial and circumferential half-waves of the resulting mode shape.

Design curves for the initial buckling load of shells with square cutouts and subjected to internal pressure are presented in figure 9a and 9b. Figure 9a shows the relation between the axial and circumferential nondimensional loading factors K_x and K_θ , respectively, for three values of the cutout or curvature parameter C , and $\alpha_b=1.068$, $\beta=2.09$, $\gamma_b=-0.186$ and $\delta_b=-0.212$. The figure indicates that the nondimensional parameters can be useful in summarizing these results in terms of nondimensional design curves. Additional information about the initial buckling loads of these shells is obtained from figure 9b. The results in this figure indicate that the initial buckling load of a shell with a cutout increases as the internal pressure increases as discussed previously. Furthermore, the results indicate that the increase in internal pressure in a shell with a cutout will result in a larger increase in the initial buckling load for larger cutouts.

Concluding Remarks

The results of an analytical study of the response of quasi-isotropic laminated shells with square cutouts subjected to axial compression and combined internal pressure and axial compression loads are presented. Results indicate that a nonlinear interaction between in-plane stresses and out-of-plane deformations near a cutout in a compression-loaded shell cause a local buckling response to occur near the cutout. For sufficiently large cutouts, the buckling response results in a stable postbuckling state consisting of large out-of-plane deformations and rapidly varying stress gradients. For

sufficiently small cutouts, the local buckling response produces enough of a disturbance to the shell to cause the overall collapse of the shell. The results indicate that an increase in the size of the cutout can cause a significant reduction in the initial buckling load of the shell and a reduction in the magnitude of the postbuckling load reduction. The results indicate that the response a compression-loaded cylinder is strongly influenced by an internal pressure load. An increase in the internal pressure causes an increase in the initial buckling load of the shell and the general instability load of the shell. Increasing the internal pressure stabilizes the shell and delays the onset of the buckling response, and increases the shell buckling loads. Numerically generated design curves based on nondimensional parameters are presented and offer a convenient format for summarizing the initial buckling loads of shells with cutouts and subjected to internal pressure and axial compression.

Acknowledgments

This work was supported by the NASA Graduate Student Researchers Program and NASA Langley Research Center, Grant Number NGT-57256.

References

- ¹Brogan, F. and Almroth, B. O., "Buckling of Cylinders with Cutouts," AIAA Journal, Vol. 8, No. 2, February 1970, pp. 236-240.
- ²Tennyson, R. C., "The Effects of Unreinforced Circular Cutouts on the Buckling of Circular Cylindrical Shells," Journal of Engineering for Industry, Transactions of the American Society of Mechanical Engineers, Vol. 90, November 1968, pp. 541-546.
- ³Starnes, J. H., "The Effect of a Circular Hole on the Buckling of Cylindrical Shells," Ph. D. dissertation, California Institute of Technology, Pasadena, California, 1970.
- ⁴Hilburger, M. W., "Numerical and Experimental Study of the Compression Response of Composite Cylindrical Shells with Cutouts," Ph. D. dissertation, University of Michigan, Ann Arbor, Michigan, 1998.
- ⁵Starnes, J. H., and Rose, C. A., "Nonlinear Response of Thin Cylindrical Shells with Longitudinal Cracks and Subjected to Internal Pressure and Axial Compression Loads," AIAA Paper No. 97-1144, April 1997.
- ⁶Brogan, F. A., Rankin, C. C., and Cabiness, H. D., "STAGS User Manual," Lockheed Palo Alto Research

Laboratory, Report LMSC P032594, 1994.

⁷Riks, E., "The Application of Newton's Method to the Problem of Elastic Stability," ASME Journal of Applied Mechanics, Vol. 39, 1972, pp. 1060-1066.

⁸Riks, E., and Rankin, C. C., "Computer Simulation of Dynamic Buckling Phenomena Under Quasi-static Loads," presented at Euromech Colloquium 317, March 1994, Liverpool, UK.

Table 1: Lamina Material Properties

E_1 , Msi	E_2 , Msi	G_{12} , Msi	ν_{12}
21.5	1.61	0.93	0.295

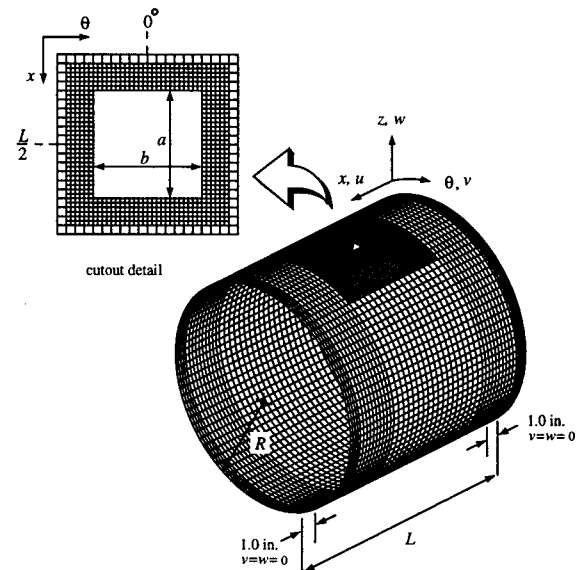


Figure 1: Typical shell model.

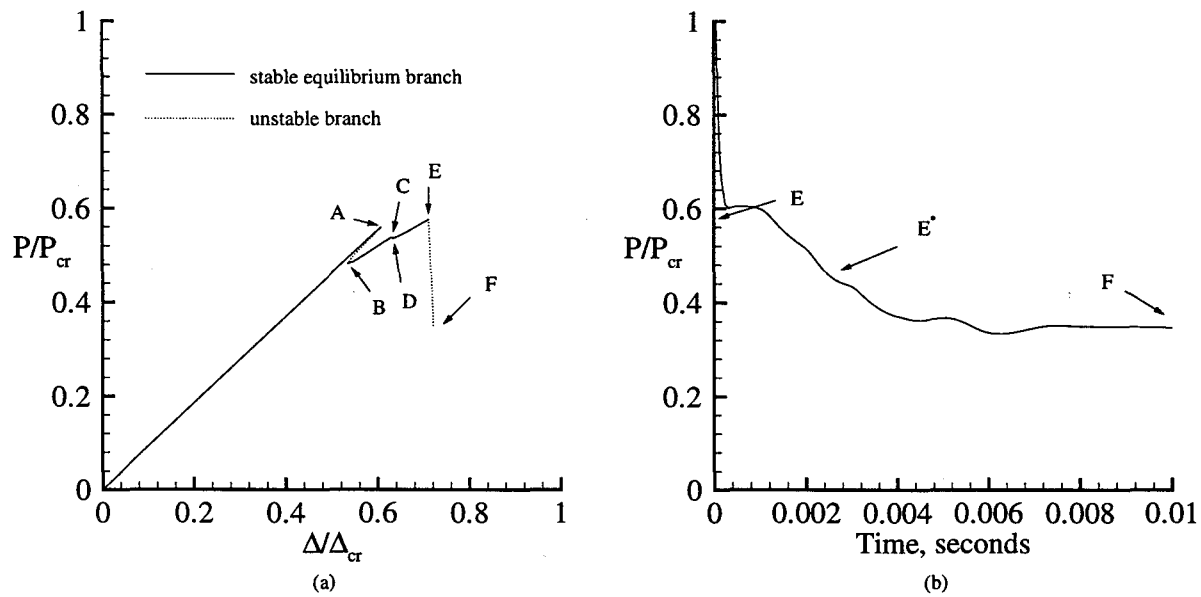


Figure 2: Compression response of a quasi-isotropic shell with a 1.0-in by 1.0-in square cutout; (a) load-shortening response, (b) load time history of the unstable collapse response associated with segment E-F in figure 2a.

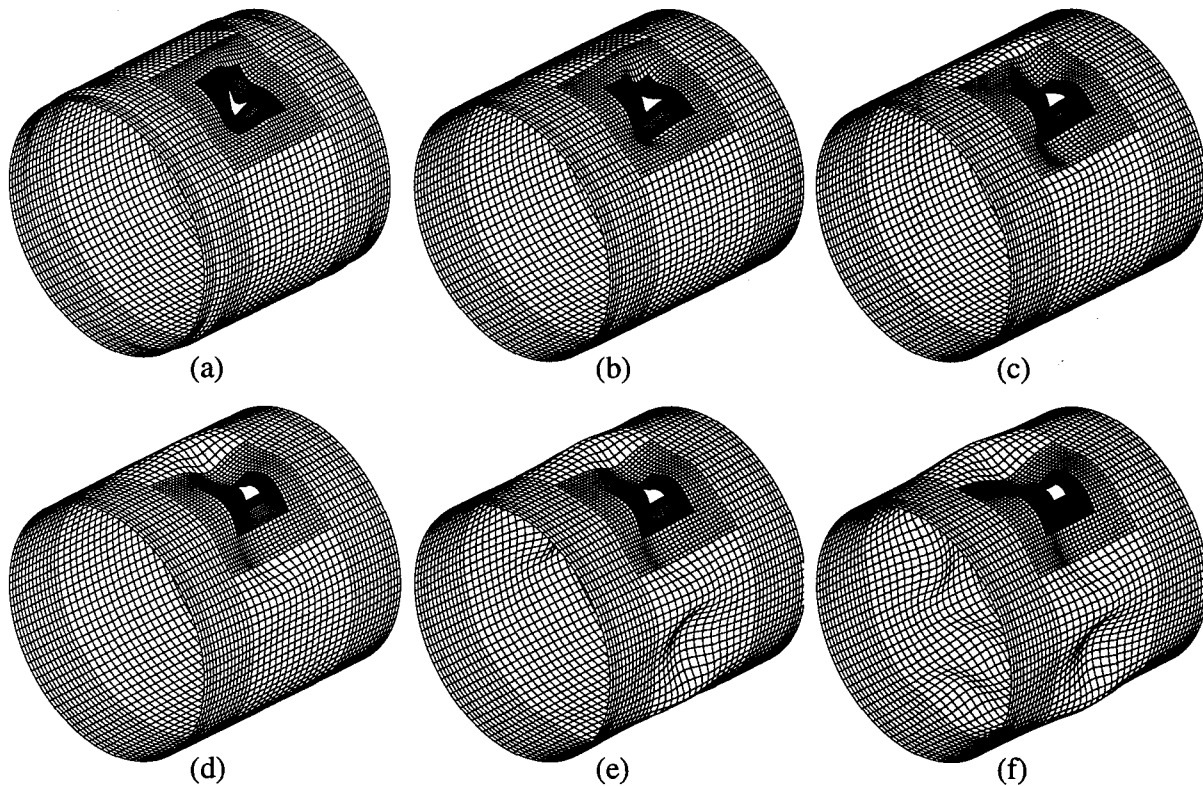


Figure 3: Selected deformation patterns for a compression-loaded quasi-isotropic shell with a 1.0-in by 1.0-in square cutout; (a) point A, (b) point B, (c) point D, (d) point E, (e) point E*, (f) point F (refer to figure 2 for selected points).

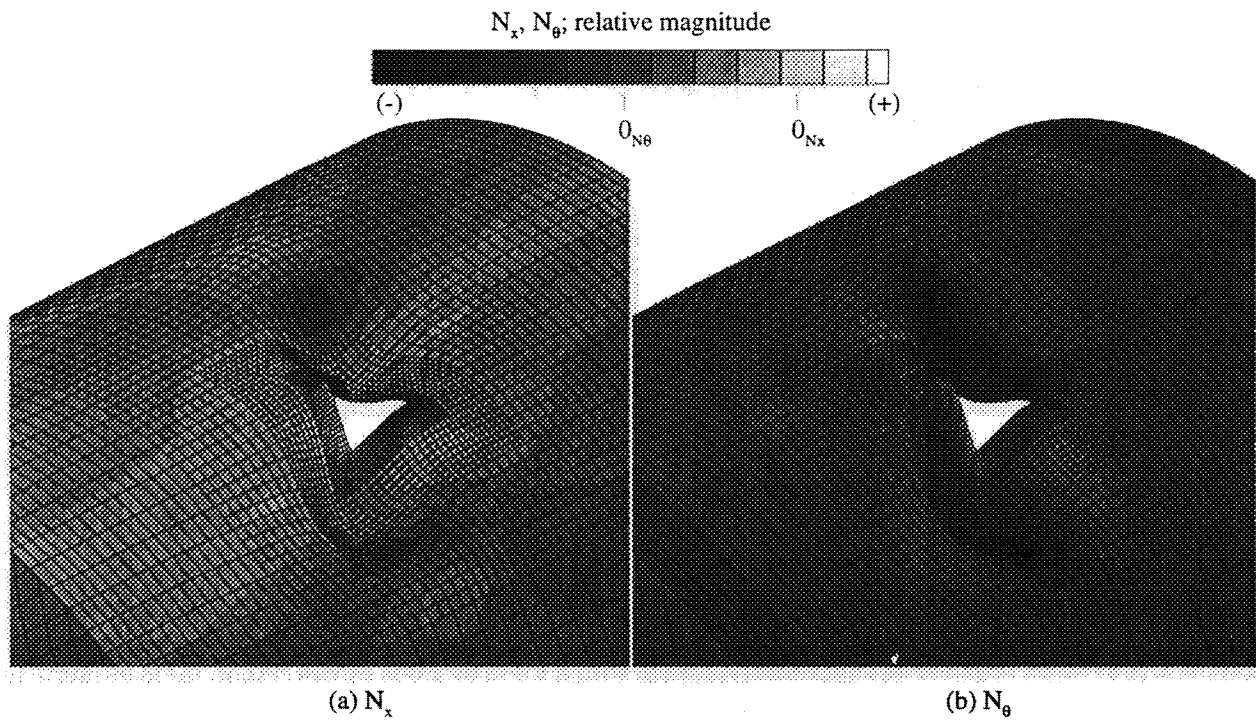


Figure 4: Buckling stress resultants for a compression-loaded quasi-isotropic shell with a 1.0-in by 1.0-in square cutout; (a) axial stress resultant (b) circumferential (hoop) stress resultant (magnified view).

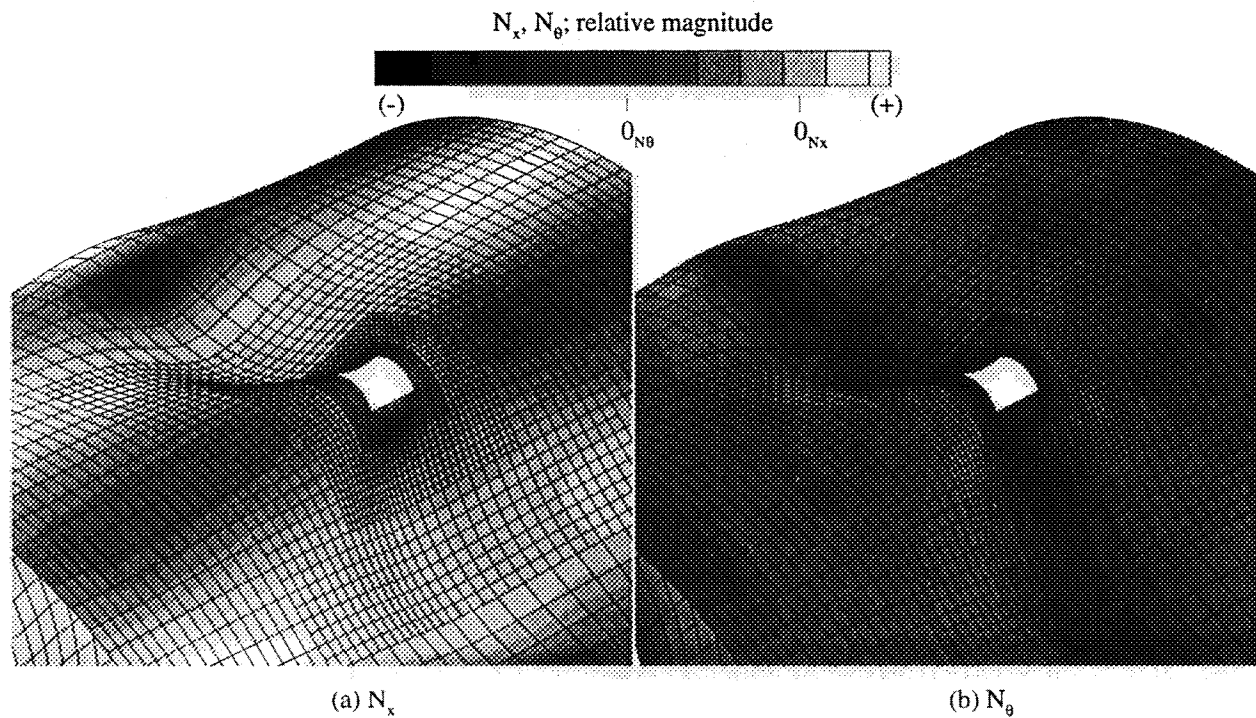


Figure 5: General instability stress resultants for a compression-loaded quasi-isotropic shell with a 1.0-in by 1.0-in square cutout; (a) axial stress resultant (b) circumferential (hoop) stress resultant (magnified view).

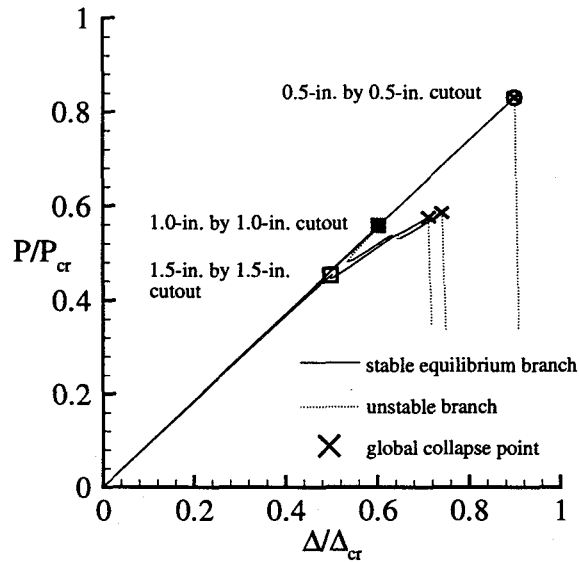


Figure 6: Effect of cutout size on the response of a quasi-isotropic shell subjected to axial compression.

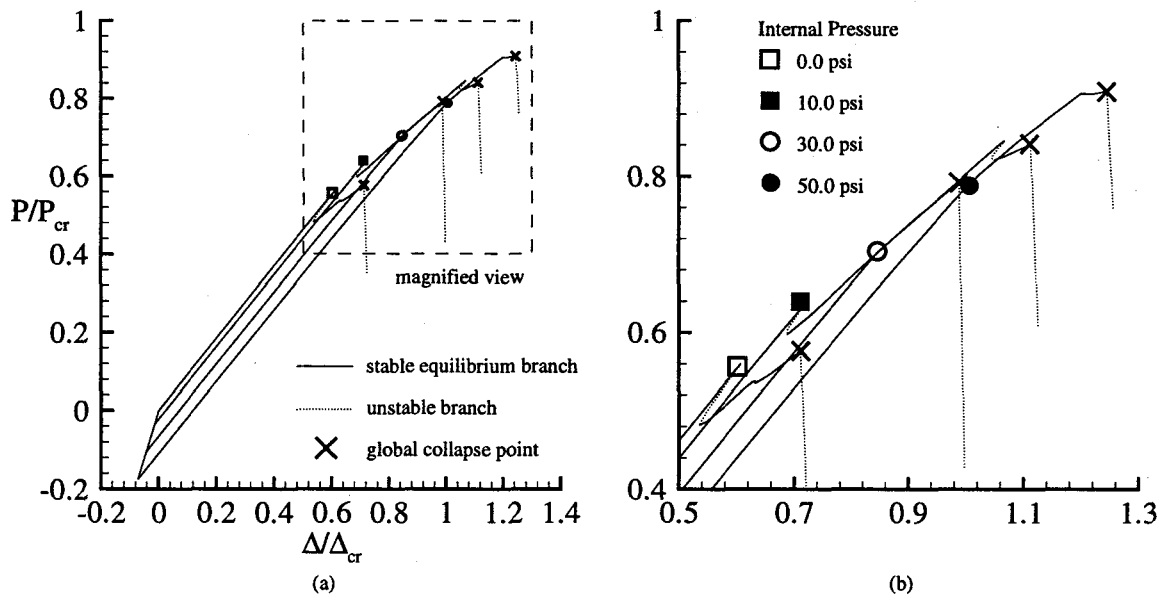


Figure 7: Effects of internal pressure on the response of a quasi-isotropic shell with a 1.0-in by 1.0-in square cutout; (a) load-shortening response, (b) magnified view of local and global buckling responses.

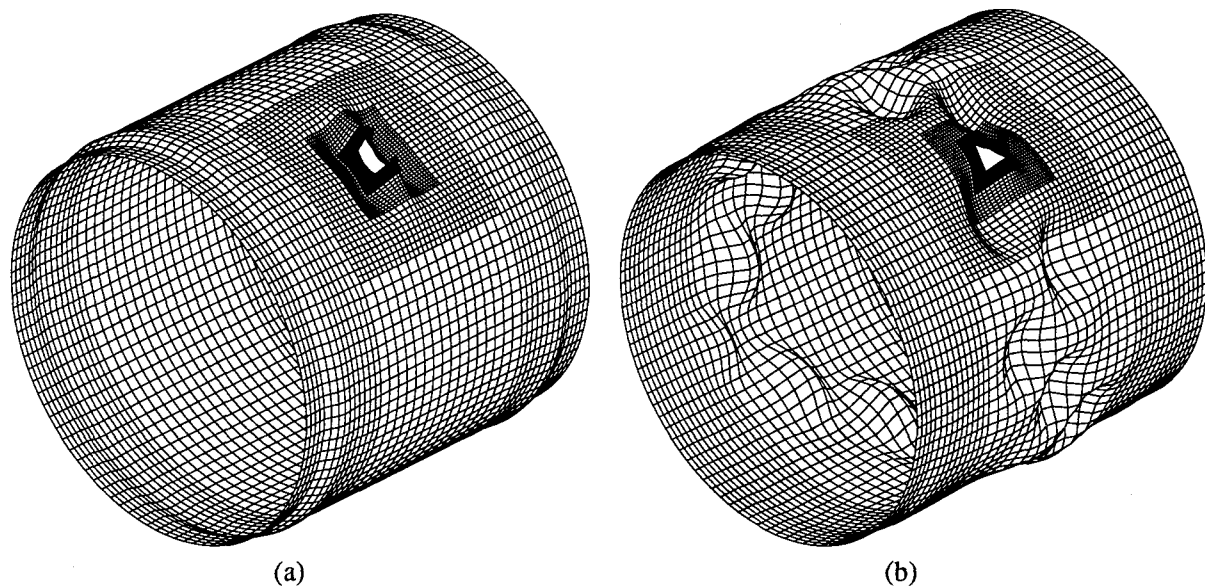


Figure 8: Selected deformation patterns for a quasi-isotropic shell with a 1.0-in by 1.0-in square cutout and subjected to 30 psi internal pressure and axial compression; (a) postbuckling deformation pattern, (b) general instability deformation pattern.

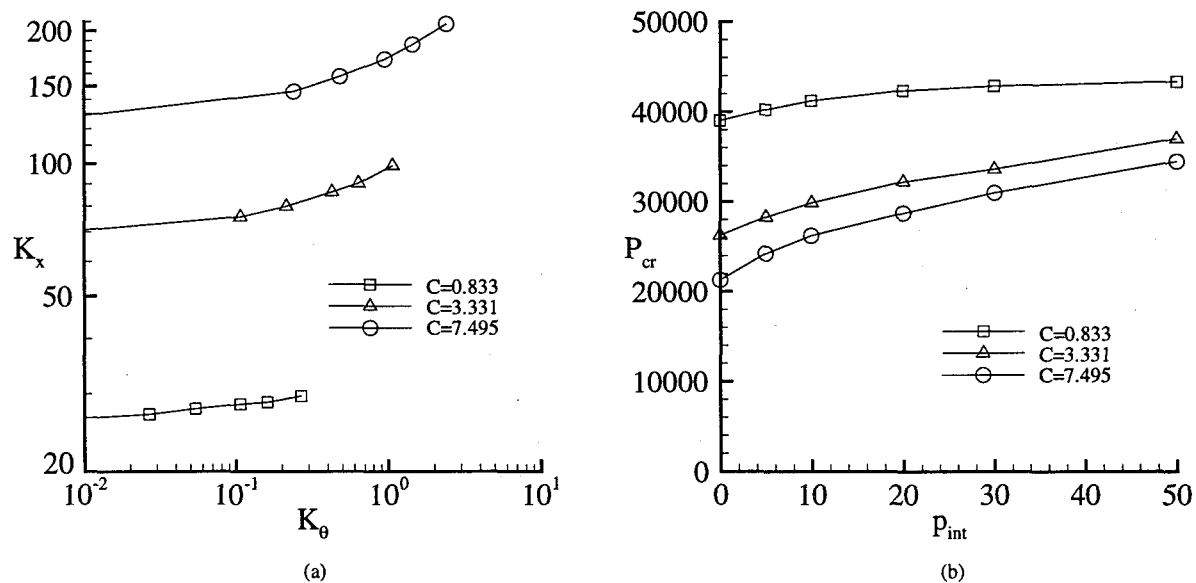


Figure 9: Design curves for the initial buckling load of a shell with a cutout and subjected to internal pressure and axial compression.